

Effect of Swirling Flow on Recirculation Ratio and Mixing in a Flameless Combustor

Haroun, H. S.^{1,*} and Eldrainy, Y. A.¹

¹Mechanical Engineering Department, Faculty of Engineering, Alexandria University, Alexandria, Egypt

Abstract: Regulations on gas turbines emissions such as NOx and CO has led to the investigation of many combustion techniques that results in a reduction in harmful emission, one of these novel techniques is flameless combustion (FC) or colorless distributed combustion (CDC). CDC has been examined under non-reacting conditions in a swirl based gas turbine flameless combustor using ANSYS Fluent at different air jet diameters and different thermal intensities for the aim of developing a design equation and a 3D flameless combustion map that includes the effect of air jet diameter and thermal intensity on recirculation ratio to allocate flameless combustion regions. A simple lab scale swirl combustor is employed for the analysis. Swirl based combustor results in about 40% increase in recirculation ration compared to non-swirl combustor and swirl combustor results in a high recirculation ratio even at high thermal intensity combustors. It is found that the optimum exit position was the central axial exit location "CA". 30% increase in the recirculation ratio was observed when separating the air jet into 2 opposite air jets each of which has half the diameter and half the mass flow rate. In addition air jet near the exit "NE" configuration showed an improvement in the recirculation ratio than the base design. Furthermore design equation is obtained to predict the appropriate air diameter that if combined with the available combustor diameter achieves a minimum recirculation ratio suitable to sustain flameless combustion.

Keywords: flameless combustion, combustor design, swirl flow, recirculation and mixing

I. INTRODUCTION

Many novel combustion techniques were investigated in order to decrease emissions in gas turbines such as rich burn –quick quench– lean burn (RQL) combustion, catalytic combustion, lean-premixed pre-vaporized (LPP) combustion, water and steam injection, however, most of them suffer from either complexity or safety issues [1, 2, 3 and 4]. Flameless combustion is safe and simple technique for emissions reduction. The key factor to achieve FC is the recirculating of POCs, which is defined as recirculation ratio (Kv) [5], which is the ratio between the recirculate product gases mass flow rate (mrec), and the inlet fresh reactants mass flow rate (ma + mf) as shown in Eq. (1).

$$Kv = mrec / (ma + mf) \quad (1)$$

[5] Suggested that the minimum value of Kv to achieve flameless combustion is 3 regardless of combustion temperature. Many researches study the effect of different geometric configurations on recirculating ratio and mixing [11-13]. Moreover, a lot of work was done to study the effect of changing the confinement size, air and fuel jets diameter as well as the change in combustor inlet conditions on Kv [14 -18]. [15] Suggested that better turbulence mixing is achieved for smaller air injection diameter and both NO and CO emissions were observed to increase with increase in air injection diameter. [16] Concluded that higher thermal intensity presents many challenges when working on flamless mode such as low residence time and low recirculation ratios. Based on these drawback [19-22] investigated a high thermal intensity swirl flow combustor operating at flameless mode. [20] Investigate both non-swirling flow and swirling flow combustors and concluded that swirling flow-Field configuration is characterized by higher flow velocities as well as high recirculated gases compared to non-swirl case. Several researches was done in order to predict a design criteria for flameless combustor, for example [21, 22] developed a distribution index that determines how well flameless mode can be achieved in a swirl combustor. In addition [23,24] developed a design equation to predict the minimum dimensions requirements needed to sustain flameless combustion, however there wasn't design equation for swirl based flameless combustors . Therefore, the present work will include a development

of a design equation for a swirl combustor. This paper will investigate the swirl combustor proposed by [19-22] in order to predict the most optimum geometric configuration.

II. METHODOLOGY

2.1 Geometric Model

The investigated swirl combustor was reported in the experimental work of [19-22]. The combustor chamber under investigation is a cylindrical chamber with diameter= $16D$ and height= $8D$, where D is diameter of air injection port. Fuel injection diameter is $D/3$ and exit diameter is $2D$, where D is $3/16$ inch. Air is injected tangentially at half the height of chamber giving a swirling air flow to the combustor the investigated combustor has combustion intensity of $36 \text{ MW/m}^3\text{-atm}$ at constant heat load of 6.25 kW is used to simulate gas turbine combustion conditions. The combustor was operated using methane as the fuel. Both methane and air were injected at ambient temperature of 300 K and the operating pressure was 1 atm . Two different configurations will be investigated, in the first configuration the exit is normal to the cylinder axis and it's denoted as "N" see fig 1a. The second arrangement has exit along the cylinder axis and denoted as 'A', see Fig. 1b.

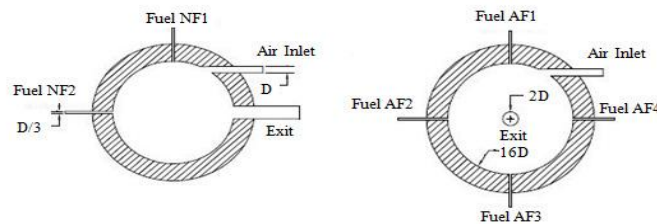


Figure 2 Schematic of the combustor for different experimental configurations [20]

2.2 Numerical Model

The flow field and species distribution are solved using a steady state, pressure based solver with finite volume discretization method, Reynolds averaged Navier - Stokes equations (RANS) and non-reacting species transport equations. Second order upwind scheme is used for pressure, momentum and species transport equations. SIMPLE is used for pressure velocity coupling. Three turbulent models were investigated; standard k-e model, realizable k-epsilon model (RKE) and Reynolds stress equations (RSM). Standard wall function is employed for all models. Two criteria for checking numerical solution convergence are assumed. First, when the monitored residuals drop below 10^{-6} for all transport equations. Second, when the monitored velocity and pressure at several points inside the domain reach steady state. ANSYS-Fluent 18.1 is used for all numerical computations. Inlet mass flow rate is applied at both air and fuel inlets. Pressure outlet is applied at the combustor exit. No-slip condition with zero heat flux is applied to all wall boundaries. Due to the complexity of the geometry tetrahedral grid was used in the present analysis. Fig. 3 shows the computational grid while Fig. 4 and Fig. 5 shows the air and fuel jet grid refinements.



Figure 3. Computational grid

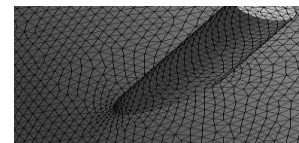


Figure 4. Air jet refinement

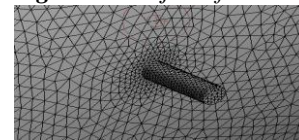


Figure 5. Fuel jet refinement

Mesh independence study is done on the "N" configuration with 5 different grid resolutions 65209, 99214, 188849, 446093 and 969952 cells. Due to the fact that the predicted axial and radial velocities for the last 2 grids (446093, 969952) were almost identical, the (446093 cells) was used for the present analysis. The second configuration "A" was performed with 5 different grid resolutions 50000, 104199, 198349, 423114 and 914014 cells. Due to the fact that the predicted axial and radial velocities for the last 2 grids (423114, and 914014) were almost identical, the (423114 cells) was used for the present analysis.

2.3 Investigated Cases

Focusing on the most effective two parameters on recirculation ratio (i.e. confinement size and air diameter), 9 operating cases are simulated by CFD ANSYS Fluent to study the relation of these critical parameters on recirculating ratio, this criteria will be done using the dimensionless parameters, air jet to combustor diameter ratio $\beta = d/D_i$, which is the ratio between the combustor air diameter to initial combustor diameter ($D_i=76.2\text{mm}$), and combustor scaling factor $Sc=D_c/D_i$, which is the ratio between the final combustor diameter and the initial combustor diameter ($D_i=76.2\text{mm}$), proposed by [23]. The 9 cases shown in Tab.1 are investigated at different air jet to combustor diameter ratios (0.0328-0.1312) and different combustor scaling factors (0.5, 1, 2). Fuel mass flow rate (mf) is kept constant at 0.000125 kg/s for all cases investigated corresponding to 6.25kw thermal input.

Table1. Investigated cases

Cases	B	Sc
1a, 1a', 1a''	0.0625	1, 0.5, 2
1b, 1b', 1b''	0.1312	1, 0.5, 2
1c, 1c', 1c''	0.0328	1, 0.5, 2

III. RESULTS

3.1 Validation of the Numerical Model

Our numerical computations are compared with the experimental measurements of [20] for the configuration "N". As seen in Fig. 5, the radial distribution of the normalized azimuthal velocity (U/U_{inlet}) was predicted at 4 different locations (L1, L2, L3, L4). Fig. 6 demonstrates the predicted radial distribution of the normalized azimuthal velocity (U/U_{inlet}) for the "N" configuration. RKE model was used in the "N" configuration. There is a good agreement between the numerical and experimental prediction for the configuration "N" for all investigated location and thus the model correctly predicts the flow field inside the 'N' combustor. Three different turbulence models were investigated for the "A" configuration. It was found that the standard k-e model could not predict the high velocity flow near the center and thus it will not be used. The RKE and the RSM could better predict that high velocity. There was an obvious difference between the numerical and the experimental results. However, the predicted radial distribution of the normalized azimuthal velocity had the same saddle shape as the experimental results and almost the same numerical predictions were seen by [20]. Due to the fact the RSM better predicts the high near center velocity it was the chosen model for our investigation.

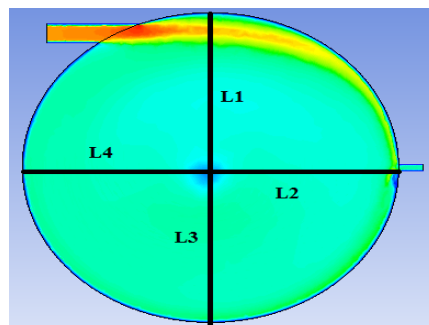
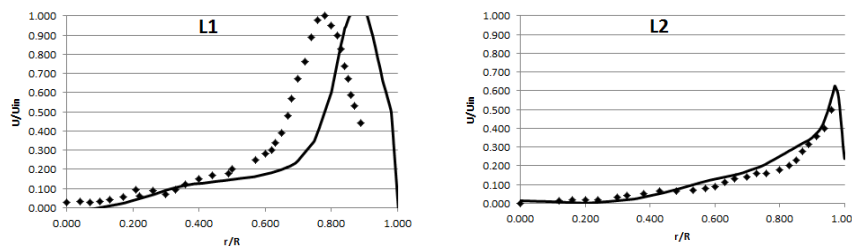


Figure 5. Calculated locations



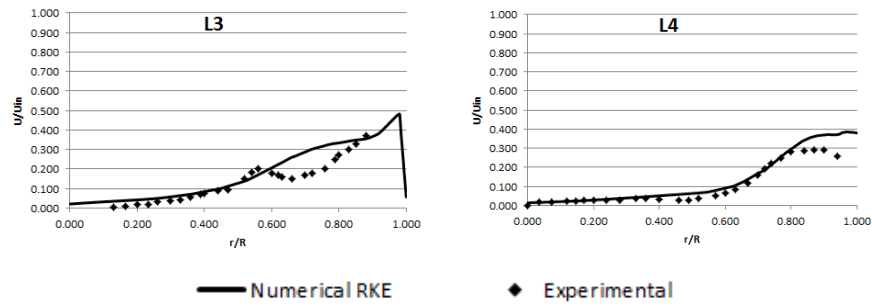


Figure 6. Numerical validation for the "N" configuration

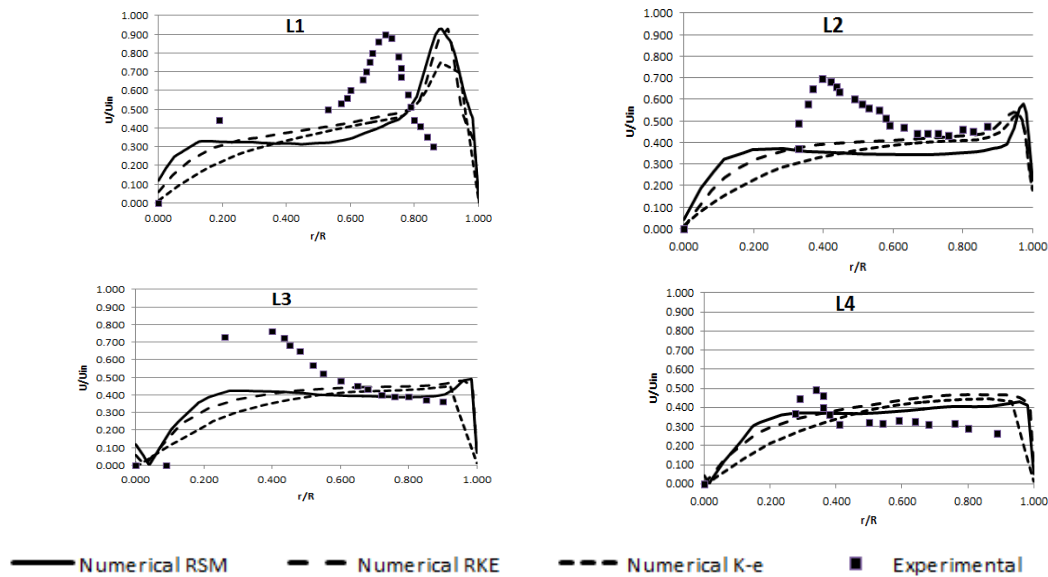


Figure 7: Numerical validation for "A" configuration

3.2 Swirl vs. non-Swirl Combustor

After investigating the two different configurations under non-reacting conditions it is seen from the velocity contour for the "N" and "A" arrangement (see Fig 8), that there is a significant difference between both arrangements in the velocity magnitude inside the combustor. Higher velocity indicates high entrainment velocity of the recirculated gases with the reactants and thus it will lead to a better mixing and thus more distributed flame and consequently low emissions. Moreover, the "N" configuration reveals a stagnant portion near the center of the combustor and thus minimal use of the combustor volume which leads to lower residence time and hence it is expected to result in a high value of CO emissions under reacting conditions.

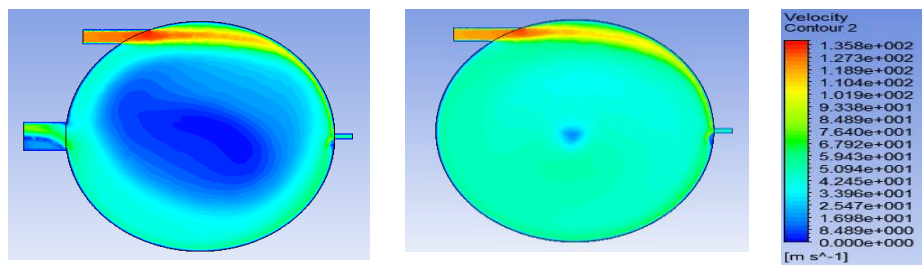


Figure 8. Predicted velocity magnitude for (a) non-swirl (b) swirl

The recirculated mass was calculated by inserting a plane which is located 0.001905m from the center of the combustor as seen in Fig 9., and then the recirculation ratio is determined as seen in Fig. 10, the predicted recirculation ratio for the "N" configuration was 9.4. On the other hand the predicted recirculation ratio for the swirl case "A" was 15.3. About 39 % increase in recirculation ratio was observed from altering the outlet location and thus the swirl model is expected to result in a high recirculation ratio sufficient to sustain a

flameless combustion mode even in high thermal intensity combustor which is the case in gas turbine engines applications especially in aviation purposes.

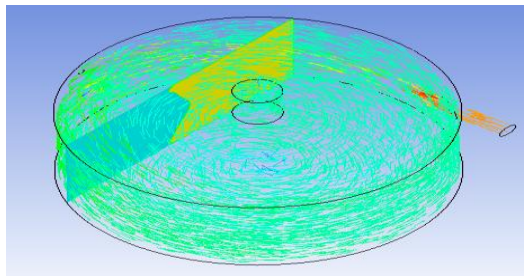


Figure 9. Recirculation ratio plane

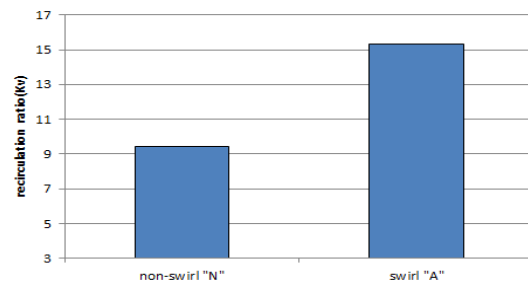


Figure 10. Recirculation ratio for "N" and "A"

3.3 Effect of air jet diameter

Fig. 11 shows the predicted velocity contour at the combustor symmetry plane for 2 different diameters $d=4.8$ and 10mm , as seen in the figure there is a significant difference in the magnitude of the velocity inside the combustor as the air jet diameter decreases to about half of its value and this indicates that better mixing will be achieved and consequently more distributed flame.

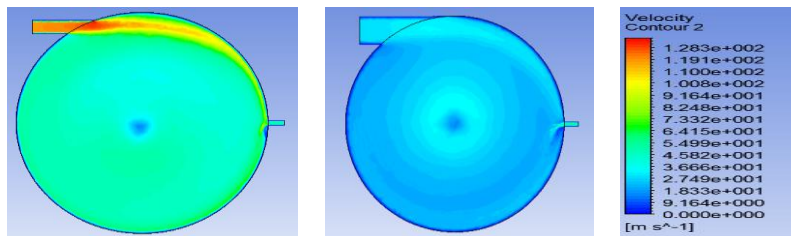


Figure 11. Predicted velocity contour at the combustor symmetry plane for 2 different diameters $d=4.8$ and 10mm

The recirculation ratio for the $d=4.8\text{mm}$ was 15.3 which indicated a high value for recirculated mass however; the recirculation ratio was 6.5 for the 10mm air jet diameter. Reducing the air jet diameter by half of its value in a swirl type combustor results in about 57% decrease in the recirculated mass inside the combustor. The high recirculated mass will increase the amount of dilution which will result in a distributed flame and consequently low combustion temperature and low NO emissions. The contour of the turbulence kinetic energy for 3 different diameters $d=2.5\text{mm}$, $d=4.8\text{mm}$, $d=10\text{mm}$. Fig. 12 indicates that reducing the air jet diameter by half of its value result in a significant change in the turbulence at the inlet and it is expected that high turbulence kinetic energy at inlet will enhance mixing of the recirculate gases with the air jet.

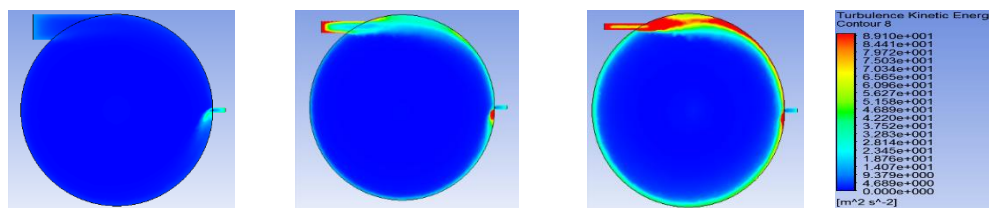


Figure 12 Predicted turbulence kinetic energy contour for $d=10\text{mm}$, $d=4.8\text{mm}$, $d=2.5\text{mm}$

3.4 Effect of confinement

decreasing the combustor diameter decrease from 76mm to 38mm , the recirculation ratio decreases about 53% , however, reducing the combustor diameter from 152mm to 76mm results in a 46% decrease in the recirculation ratio and this percent is reduced as the diameter increases from ($D_c = 152$ to 304) to about 43% . It is concluded that as the thermal intensity increase the recirculation ratio decrease taking into consideration that the percentage of decrease is more significant at the higher thermal intensity combustors than lower ones and this may be due to the proximity of the combustor walls to the outer edges of the jets which prevents a high ratio of recirculating gases to be entrained. Fig. 13 shows the % of decrease in the recirculation ratio for different combustor diameters at a constant air jet diameter of $d=4.8\text{mm}$.

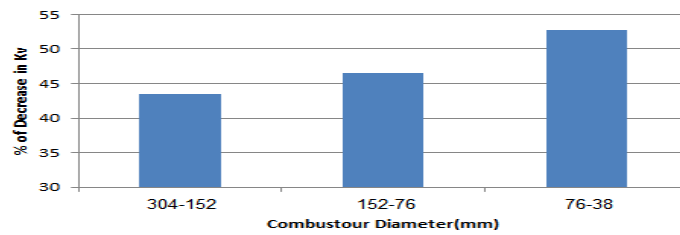


Figure 13. % of decrease in the kv for different combustor diameters at d=4.8mm.

Reducing the confinement to half of its value at a constant diameter (d=4.8mm) did not reveal a substantial increase in the turbulence kinetic energy as the case of reducing the diameter to half of its value, and this can be shown in Fig. 14. The energy contained in the recirculation zone eddies depends on the change in the air jet diameter but does not depend on the confinement size.

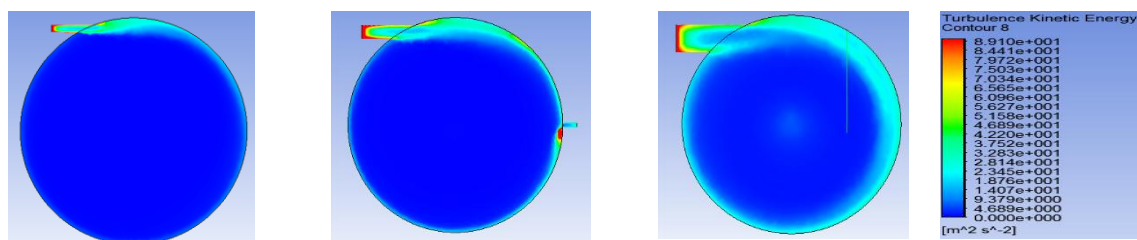


Figure 14 Predicted turbulence kinetic energy contour for d=10mm, d=4.8mm, d=2.5mm

3.5 Changing the axial exit location

Numerical investigations were performed on configuration "A" to evaluate the impact of the changing the axial exit location on the recirculation inside the combustor. Four exit axial locations were investigated, left axial "LA", right axial "RA", down axial "DA" and up axial "UA" and they were compared with the base design with the center axial "CA". For each of these axial locations the velocity flow field was obtained and its behavior was analyzed. The obtained velocity fields are shown in Fig. 15. From the velocity contours plot, it is seen that "LA" configuration reveals a stagnant portion near the center of the combustor, where the flow velocity for the center part is almost zero. Such flow behavior indicates minimal use of the combustor volume which leads to lower residence time and hence it's expected to result in a high value of CO emissions under reacting conditions. The calculated recirculation ratio for that configuration "LA" was less than the base design "CA" by an about 23%. other configurations "RA", "UA", "DA" also indicate that center stagnate region which correspond to minimal use of the combustor and thus it's concluded that the optimum position was the base design configuration with a central axial exit location "CA". The calculated recirculation ratio for the investigated configurations can be seen in Fig 15.

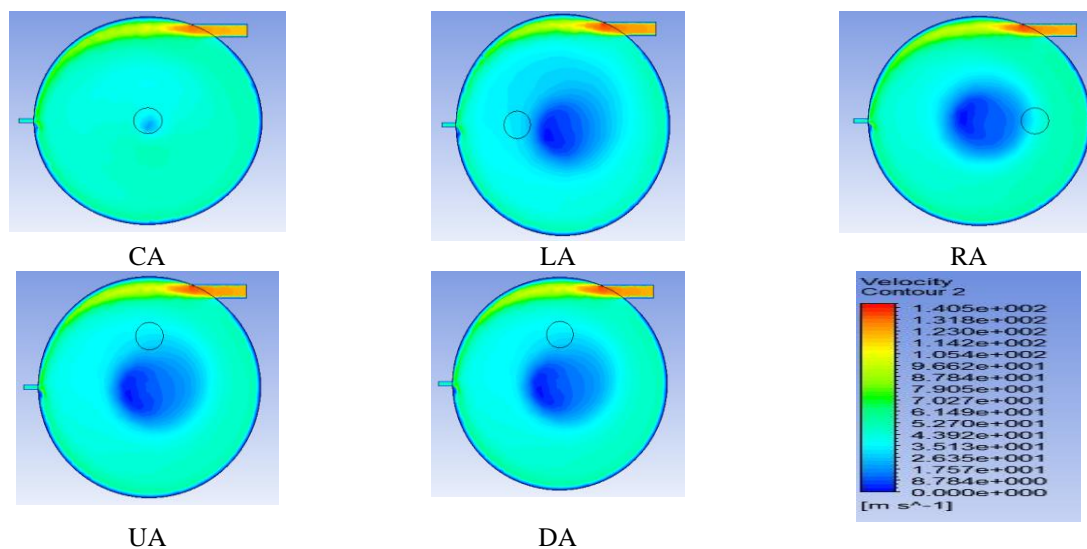


Figure 15. Predicted velocity contour for different axial exit configuration

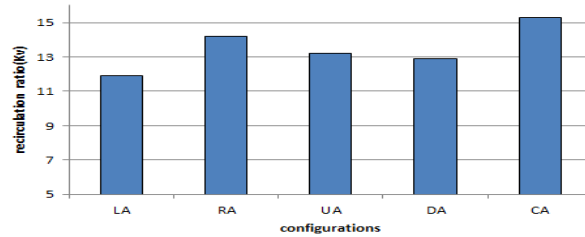


Figure 16. Calculated kv for the investigated configurations

3.6 Effect of air jets configurations

Numerical investigation was done to study the effect of separating the total mass flow rate between 2 jets each jet has half the value of the base design diameter. The obtained velocity fields are shown in Fig. 17.

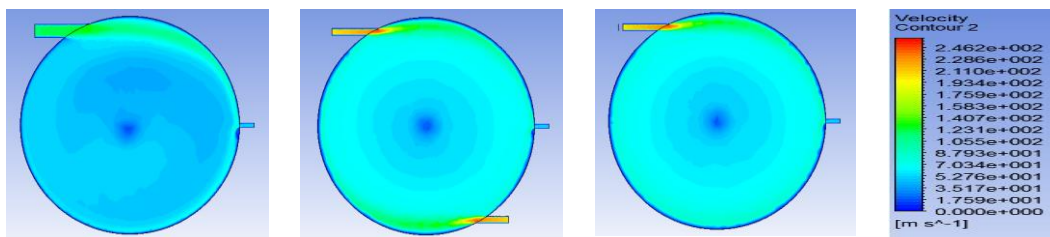


Figure 17. Velocity contour for different air jets configurations at half diameters

From the velocity contours plot, it is seen that there is a significant change in the velocity magnitude inside the combustor for the 2 half diameter jets configurations. Although each jet has half the mass flow rate, the effect of changing the diameter is much higher than changing the mass flow rate and that explains the significant difference between the configurations. The calculated recirculation ratio for the configurations can be seen in Fig. 18.

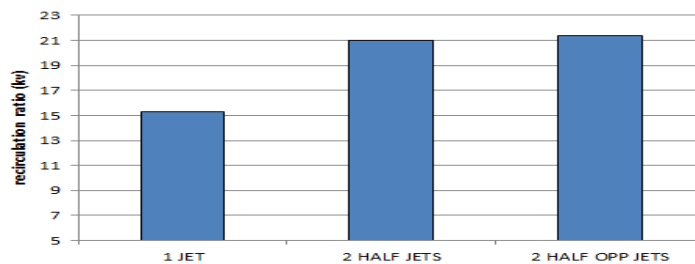


Figure 18. Calculated kv for different air jets configuration at half diameters

Deeper jet penetration was observed for the 2 jets and 2 opposite jets and about 30% percent improvement in the recirculation ratio was observed for the 2 opposite jets where each jet is half the diameter of the base design.

3.7 Design equation

For the aim of design a swirl based flameless combustor, it is important to know the appropriate air diameter that if combined with the available combustor diameter achieves a minimum value of recirculation ratio suitable to sustain flameless combustion. The minimum recirculating ratio for flameless combustion as proposed by [5] is 3 regardless of furnace temperature above 800 °C, so developing a design equation that obtain the minimum combustor dimensions (air jet diameter and combustor diameter) would be beneficial for a preliminary design of a swirl based flameless combustor.

Thus the results of the 9 cases (see Tab.2) are plotted in the form of a 3D curve, to study the relation between the three main factors (recirculation ratio, air diameter and confinement) and a flameless combustion map in addition to a design equation was developed. Fig. 19 demonstrates the relation between air diameter ratio (y axis), combustor scaling factor (x axis) and recirculation ratio (z axis). Red color (region A) indicates that the combustor is expected to operate in a flameless mode and the reaction in that region is expected to be highly distributed under reacting conditions and thus the lowest emissions could be on region A. subsequently yellow color (region B) indicates that the combustor will work on flameless mode and the reaction is less distributed and the emissions could be higher than region A, light blue color (region C) indicates that the

combustor may or may not operate at a flameless mode depending on its excess air ratio, where the minimum recirculation ratio to achieve flameless mode depends on it, finally the dark blue color (region D) indicates that the combustor won't operate at a flameless mode where that region has a recirculating ratio below 3. Fig. 20 demonstrates the relation between air diameter ratio (y axis), combustor scaling factor (z axis) and recirculation ratio (x axis) on a 3D curve and by fitting that curve equation 3 is obtained.

$$S_c = a + bK_v + c\beta + dK_v^2 + eK_v\beta + f\beta^2.$$

A=-0.1681, b=0.00872, c=2.802, d=5.134*10⁻⁵, e=0.9362, f=-1.288

By substituting with the minimum recirculation ratio that sustains flameless combustion (Kv=3), Eq. 3 can approximately estimate the following:

- 1) The most appropriate (maximum) air jet diameter for a given combustor diameter to achieve flameless combustion.
- 2) the most appropriate (minimum) combustor diameter for a given air jet diameter to achieve flameless combustion.

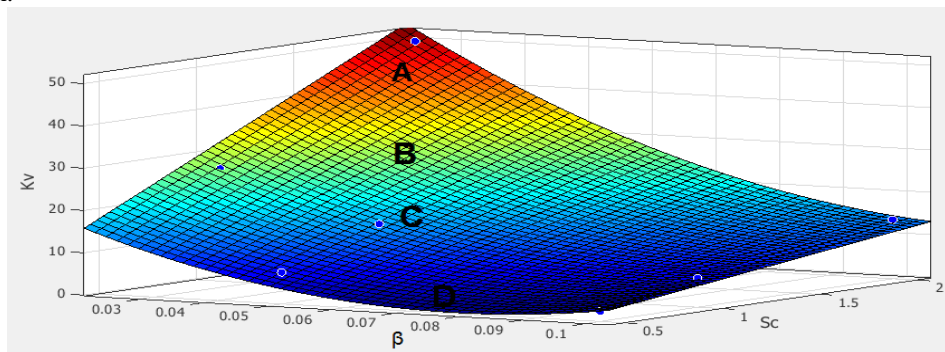


Figure 19. Flameless Combustion Map.

Fig. 21 demonstrates the relation between air diameter and combustor diameter at a constant recirculation ratio 3, corresponding to the minimum value in order to achieve flameless combustion. It is concluded that as the combustor diameter increases (increase confinement) the maximum air diameter needed to achieve flameless combustion increases. This may be due to the fact that the higher confinement will compensate the need of a lower diameter in order to achieve a given recirculation ratio. It is also found that air jet diameter should be at most about 20% of the combustor diameter in order to achieve flameless combustion. It was found in non-swirls combustor that the air jet diameter should be at most 10 % of the combustor diameter in order to achieve flameless combustion [24] and that explain the fact that sustaining a flameless combustion in a swirl based combustor is much easier than sustain it in a non-swirl combustor, where the minimum air jet diameter requirements increase to about 10% in swirl based combustor.

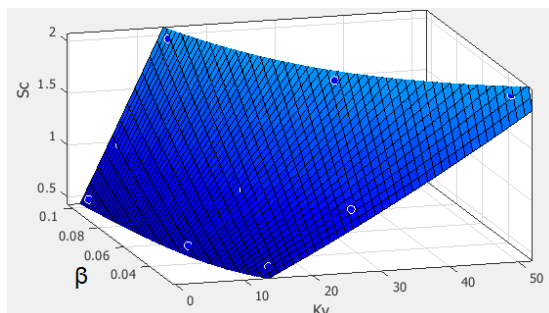


Figure 20. Relation between β , Sc and K_v

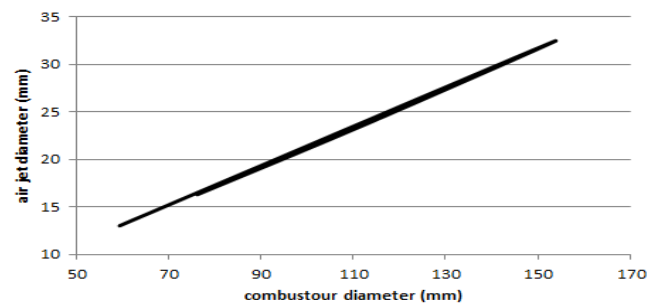


Figure 21. Relation between d and D_c at ($K_v=3$)

Table 2: K_v at different cases

Case	K_v	Case	K_v	Case	K_v
1a	15.3	1a'	7.23	1a''	28.69
1b	6.6359	1b'	2.133	1b''	13.7
1c	26.32	1c'	14.27	1c''	49.7

IV. CONCLUSION

For the aim of developing a design criteria that includes the effect of thermal intensity and air diameter on recirculation ratio and mixing, CDC has been examined under non-reacting conditions in a swirl based gas turbine flameless combustor using ANSYS Fluent the following conclusions were found:

- 1) Swirl based combustor results in about 40% increase in recirculation ratio compared to non-swirl combustor.
- 2) Reducing the air jet diameter by half of its value in a swirl type combustor results in about 57% decrease in the recirculated mass inside the combustor and that percentage increase at higher thermal intensities combustors
- 4) It is found that the optimum exit position was the base design configuration with a central axial exit location "CA" since it gives the highest recirculation ratio
- 5) 30% increase in the recirculation ratio when separating the air jet in 2 opposite air jets each of which has half the diameter and half the mass flow rate. 2 opposite half diameters air jets is expected to achieve a great reduction than the base design under reacting conditions.
- 7) Design equation is obtained in aim to predict the most appropriate air diameter that if combined with the available combustor diameter achieves a minimum recirculation ratio suitable to sustain flameless combustion.

$$S_c = a + bK_v + c\beta + dK_v^2 + eK_v\beta + f\beta^2$$

REFERENCES

- [1]. Lefebvre A.H., Gas Turbine Combustion, 2nd ed. (1998). Taylor and Francis.
- [2]. Khidr, K. I., Eldrainy, Y. A., & EL-Kassaby, M. M. (2017). Towards lower gas turbine emissions: Flameless distributed combustion. *Renewable and Sustainable Energy Reviews* 67: 1237-1266.
- [3]. Costa, Mário, et al. (2009). Experimental investigation of a novel combustor model for gas turbines. *Journal of Propulsion and Power* 25.3: 609-617.
- [4]. Daggett D., Fucke L., Hendricks R., Eames D. (2004). Water injection of commercial aircraft to reduce airport emissions. *Proc. 40th AIAA/ASME/SAE/ASEE joint propulsion conference and exhibit*.
- [5]. Wünnig, J. A., and J. G. Wünnig (1997). Flameless oxidation to reduce thermal NO-formation. *Progress in energy and combustion science* 23.1: 81-94.
- [6]. Xing, Fei, et al. (2017). Flameless combustion with liquid fuel: A review focusing on fundamentals and gas turbine application. *Applied energy* 193: 28-51.
- [7]. LiP, MiJ, DallyBB, WangF, WangL, LiuZ, etal. (2011). Progress and recent trend in MILD combustion. *Sci China Technol Sci*: 54:255-69.
- [8]. Choi, Gyung-Min, and Masashi Katsuki (2001). Advanced low NOx combustion using highly preheated air. *Energy conversion and Management* 42.5: 639-652.
- [9]. Rao, Arvind G., and Yeshayahou Levy (2010). A new combustion methodology for low emission gas turbine engines. *8th HiTACG conference*, Poznan.
- [10]. Hejie L., Ahmed E., Andrei E. (2009). Effect of exhaust gas recirculation on NOx formation in premixed combustion system/ *Proc. 47th AIAA aerospace sciences meeting including the new horizons forum and aero- space exposition*.
- [11]. Kumar, Sudarshan, P. J. Paul, and H. S. Mukunda (2005). Investigations of the scaling criteria for a mild combustion burner. *Proc. of the combustion institute* 30.2: 2613-2621.
- [12]. Khalil, Ahmed EE, Vaibhav K. Arghode, and Ashwani K. Gupta. (2013). Novel mixing for ultra-high thermal intensity distributed combustion. *Applied Energy* 105: 327-334.
- [13]. Arghode, Vaibhav K., and Ashwani K. Gupta. (2010). Effect of flow field for colorless distributed combustion (CDC) for gas turbine combustion. *Applied Energy* 87.5: 1631-1640.
- [14]. Li, G., Stankovic, D., Overman, N., Cornwell, M., Gutmark, E., & Fuchs, L. (2006). Experimental study of flameless combustion in gas turbine combustors. *Proc. 44th AIAA Aerospace Sciences Meeting and Exhibit*.
- [15]. Arghode, V. K., & Gupta, A. K. (2011). Development of high intensity CDC combustor for gas turbine engines. *Applied Energy* 88.3: 963-973.
- [16]. Arghode, V. K., & Gupta, A. K. (2011). Investigation of forward flow distributed combustion for gas turbine application. *Applied Energy* 88.1: 29-40.
- [17]. Verissimo, A. S., Rocha, A. M. A., & Costa, M. (2011). Operational, combustion, and emission characteristics of a small-scale combustor. *Energy & Fuels* 25.6: 2469-2480.
- [18]. Verissimo, A. S., Rocha, A. M. A., & Costa, M. (2013). Importance of the inlet air velocity on the establishment of flameless combustion in a laboratory combustor. *Experimental thermal and fluid science* 44: 75-81.
- [19]. Khalil, A. E., & Gupta, A. K. (2011). Swirling distributed combustion for clean energy conversion in gas turbine applications. *Applied Energy*, 88(11), 3685-3693.
- [20]. Khalil, Ahmed EE, and Ashwani K. Gupta. (2014). Swirling flowfield for colorless distributed combustion. *Applied Energy* 113: 208-218.
- [21]. Khalil, A. E., & Gupta, A. K. (2014). Velocity and turbulence effects on high intensity distributed combustion. *Applied Energy*, 125, 1-9.
- [22]. Khalil, A. E., & Gupta, A. K. (2014). Towards distributed combustion for ultra low emission using swirling and non-swirling flowfields. *Applied energy*, 121, 132-139.
- [23]. Khalil, H. M., Eldrainy, Y. A., Saqr, K. M., & Abdelghaffar, W. A. (2018). "Evaluation criteria for a flameless combustor based on recirculation and mixing-A CFD approach", *Acta Astronautica*.
- [24]. Haroun, H. S. and Eldrainy, Y. A. (2019). "Design and Investigation of Flameless Combustor based on 3D Analysis ", *11th Mediterranean combustion Symposium (MCS11)*, Spain.